From cooperative paramagnetism to Néel order in $Y_2Ru_2O_7$: Neutron scattering measurements

J. van Duijn,[1,2,3] N. Hur,[4] J. W. Taylor,[2] Y. Qiu,[5] Q. Z. Huang,[5] S.-W. Cheong,[4] C. Broholm,[1,5] and T. G. Perring[2]

[1]*Department of Physics and Astronomy, The Johns Hopkins University, Baltimore, Maryland 21218, USA*

[2]*ISIS Facility, Rutherford Appleton Laboratory, Chilton, Didcot, OX11 0QX, United Kingdom*

[3]*Departamento Química Inórganica I, Facultad de Ciencias Químicas, Unversidad Complutense de Madrid, Madrid, E-28040, Spain*

[4]*Rutgers Center for Emergent Materials and Department of Physics and Astronomy, Rutgers University,*
Piscataway, New Jersey 08854, USA

[5]*NIST Center for Neutron Research, National Institute of Standards and Technology, Gaithersburg, Maryland 20899, USA*

Spin correlations in the pyrochlore antiferromagnet $Y_2Ru_2O_7$ with Curie-Weiss temperature $\Theta_{CW}* -1100$ K and critical temperature $T_N = 77$ K were examined through neutron scattering. For $T_N < T < \Theta_{CW}/3$ the data show spin relaxation with a rate $\hbar\Gamma = 1.17(9)k_B T$. For $T < T_N$ spectral weight moves to higher energies with substantial changes up to $4k_B T_N$. For $T \ll T_N$ there is a $\Delta = 11(1)$ meV energy gap and a pronounced spectral maximum at 19.7 meV. Throughout the temperature range examined, the wave vector dependence of inelastic scattering exhibits a broad peak for $Qd \approx 3.8$ (d is the Ru-Ru spacing) consistent with dipolar spin correlations.

PACS number(s): 76.50.+g, 75.40.Gb, 75.50.Ee

In the pyrochlore structure, with general formula $A_2B_2O_7$, both the A (trivalent rare earth ions) and B (tetravalent transition metal ions) site ions form a lattice of corner-sharing tetrahedra.[1] Weakly connected and nonbipartite, this lattice produces anomalous frustrated magnetism when populated by spins with near-neighbor antiferromagnetic (AFM) interactions.[2] For classical spin vectors the lowest-energy states form a manifold characterized by zero magnetization on every tetrahedron.[3] Rather than Néel order for $T \approx |\Theta_{CW}|$, pyrochlore magnets remain disordered to much lower T, where the collective properties are governed by quantum fluctuations, thermal fluctuations, and subleading interactions.[4–6] Examples of low-T states that have been reported are spin glasses,[7] spin liquids,[8,9] and magnetoelastically induced Néel order.[10,11]

$Y_2Ru_2O_7$ is a Mott insulator with $S = 1$ Ru^{4+} spin and a large negative Curie-Weiss temperature $\Theta_{CW} \approx -1100$ K.[12–15] Specific heat and susceptibility data indicate a magnetic phase transition at $T_N = 77$ K.[13,16,17] Diffraction measurements show that the transition is to a long-range-ordered (LRO) AFM $q = 0$ structure.[18] The total spin per tetrahedron vanishes so this state is indeed a specific member of the low-energy AFM pyrochlore manifold. Here we report a neutron scattering experiment probing the anomalous spin dynamics of $Y_2Ru_2O_7$. The measurements reveal that AFM spin correlations are established at temperatures at least as high as 300 K and evolve little upon cooling. The spin relaxation rate, however, decreases linearly in T according to $\hbar\Gamma = 1.17k_B T$, consistent with proximity to quantum criticality. However, Néel order yields an 11(1) meV gap in the excitation spectrum and moves spectral weight to a 19.7 meV peak.

A powder sample of $Y_2Ru_2O_7$ was synthesized using the solid state reaction method. A mixture of Y_2O_3 and RuO_2 in proper molar ratio was prereacted at 850 °C for 15 h in air and then ground and pressed to pellets. The pellets were sintered at 1000–1200 °C in air with intermediate grindings to improve homogeneity. Powder neutron diffraction data

were collected using the BT1 diffractometer at NIST. Rietveld analysis confirmed the cubic pyrochlore structure above and below T_N with space group $Fd\bar{3}m$ (227) and lattice parameter $a = 10.128\ 24(2)$ Å at $T = 10$ K. The analysis also revealed 0.044(2) wt % unreacted Y_2O_3. Inelastic neutron scattering experiments were performed on the MARI spectrometer at the ISIS Facility and the DCS spectrometer at NIST. On MARI we used an incident energy $E_i = 150$ meV for an elastic energy resolution of 3.5 meV. The phonon contribution to the neutron scattering was subtracted by scaling the spectrum measured at high wave vectors, where the magnetic response is negligible, using the DISCUS package.[19] This program uses a Monte Carlo method to calculate a wave-vector-dependent scaling factor, which showed no significant energy dependence. For the DCS experiment we used 13.09 meV neutrons, which produced an elastic energy resolution of 0.77 meV. For both experiments count rates were normalized using $Y_2Ru_2O_7$ Bragg peaks. This produced absolute measurements of $\tilde{I}(Q,\hbar\omega) = (\gamma r_0)^2 |(g/2)F(Q)|^2 2\tilde{\mathcal{S}}(Q,\hbar\omega)$ to an overall scale accuracy of 20%. Here $\gamma = -1.913$ and $g \approx 2$ are gyromagnetic ratios for the neutron and Ru^{4+}, respectively, $r_0 = 2.82$ fm is the classical electron radius, and $F(Q)$ is the magnetic form factor. Lacking specific information for Ru^{4+}, we used the Ru^+ form factor for model comparison.[20] $\tilde{\mathcal{S}}(Q,\hbar\omega)$ is the spherically averaged dynamical correlation function.[21]

The magnetic neutron scattering cross section for $Y_2Ru_2O_7$ powder is shown in Fig. 1 for $T = 15$, 50, and 90 K. For $T > T_N = 77$ K the spectra indicate short-range AFM correlations and a spin relaxation response with a relaxation rate $\Gamma \sim k_B T/\hbar$. Upon cooling below T_N, spectral weight moves to higher energies, with modifications up to $4k_B T_N$. Figure 2 shows that the wave vector dependence of the inelastic magnetic scattering is all but unaffected by the comprehensive rearrangement of the excitation spectrum. Indeed the Q dependence of scattering changes little below room temperature. These data are consistent with frustrated interactions
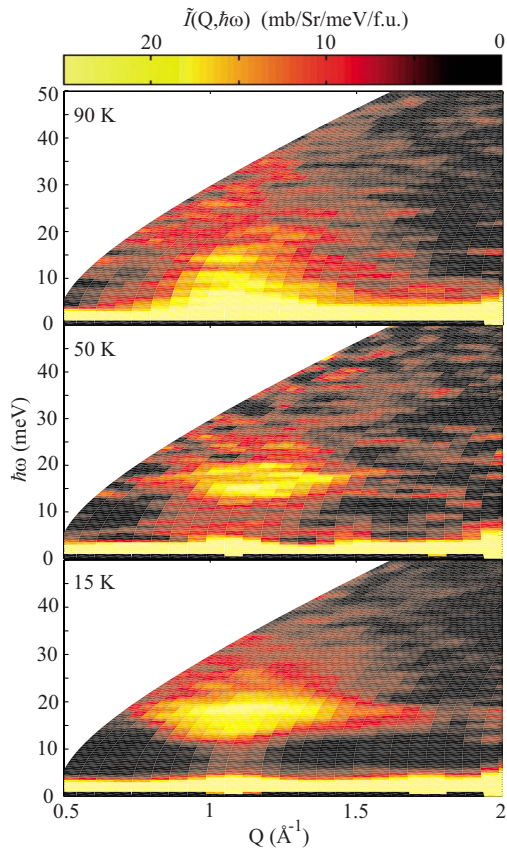
FIG. 1. (Color online) Normalized magnetic neutron scattering intensity $\tilde{I}(Q,\hbar\omega)$ for a $Y_2Ru_2O_7$ powder sample at $T=90$ (top), 50 (middle), and 15 K (bottom). Phonon scattering was subtracted as described in the text. The elastic intensity is dominated by nuclear scattering.

FIG. 2. (Color online) Q integrated (a)–(d) and $\hbar\omega$ integrated (e)–(h) inelastic neutron scattering intensity of $Y_2Ru_2O_7$ taken at $T=200$, 90, 50, and 15 K. Ranges of integration are indicated in each column. The (solid and dashed) lines show fits to the data described in the text. Lines in (a) and (b) account for the finite sampling of Q-ω space and partially resolved elastic scattering. Solid squares in (h) are normalized energy-integrated data from DCS covering the energy range from 2 to 8 meV.

with an energy scale set by $|\Theta_{CW}|*1100$ K that establish a low-energy manifold of near-degenerate states with a characteristic interatomic "form factor."[22]

The Fourier transform of six collinear antiferromagnetically correlated spins on the vertexes of a hexagon provide a reasonable account of the **Q** dependence of inelastic scattering in $ZnCr_2O_4$ over a wide temperature range.[22,23] We have calculated a spherical average of this function for comparison with the powder data in Fig. 2(h) (dashed line). The close correspondence of the calculated peak width and position with the data indicates that antiferromagnetically correlated hexagons are also prevalent in $Y_2Ru_2O_7$.

A rigorous understanding of spin correlations in the pyrochlore antiferromagnet is now emerging from theoretical work. For classical spins ($S\to\infty$), any spin configuration on the pyrochlore lattice where all tetrahedra have zero net moment is a ground state. Higher-order spin wave theory ($1/S$ expansion) and the Schwinger-boson large-N expansion show that quantum fluctuations favor states that maximize the number of flippable spins. Henley argues that this leads to selection of collinear spin configurations so the low-energy physics can be represented by an effective Ising model with a collective spin axis.[4] The selected spin configurations are further characterized by a zero-divergence co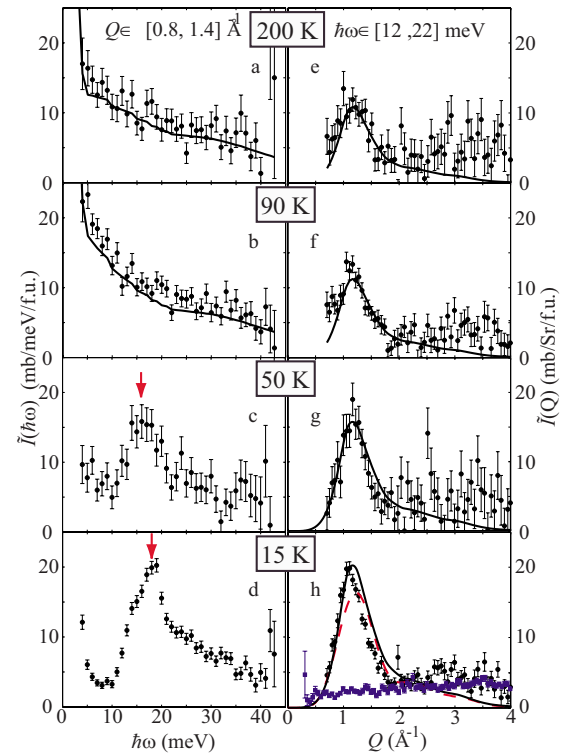ndition for a polarization field defined on the dual diamond lattice of bonds. The effective Ising model favors AFM hexagons,[24] which may account for their prevalence in $ZnCr_2O_4$ and $Y_2Ru_2O_7$. The corresponding spin correlation function $\mathcal{S}(\mathbf{Q})$ is, however, not the Fourier transform of a finite-size object as it has infinitely sharp features (pinch points) associated with the divergence-free condition.[4,5] Isakov *et al.* derive an analytic expression for $\mathcal{S}(\mathbf{Q})$ from the large-N approximation, which accurately reproduces results from Monte Carlo simulations of the classical spin Heissenberg model.[5] The solid line in Figs. 2(e)–2(h) is the spherical average of this expression multiplied by the squared Ru^+ form factor.[20] The discrepancy at high Q may result from residual phonon contributions to the experimental data and/or the ruthenium magnetic form factor employed in the model calculation. With the overall amplitude as the sole adjustable parameter the large N result provides an excellent account of the data. Note though that the spherical averaging inherent to powder neutron scattering precludes insight on finer details such as the predicted pinch points. Indeed, there are substantial differences between $\mathcal{S}(\mathbf{Q})$ from the large-N expansion and $\mathcal{S}(\mathbf{Q})$ for antiferromagnetic hexagons. Single-crystal data will be needed to determine which is more appropriate for $Y_2Ru_2O_7$. At elevated temperatures defects should appear in the form of monopoles[4] that give rise to a finite divergence of the polarization field and broadening of
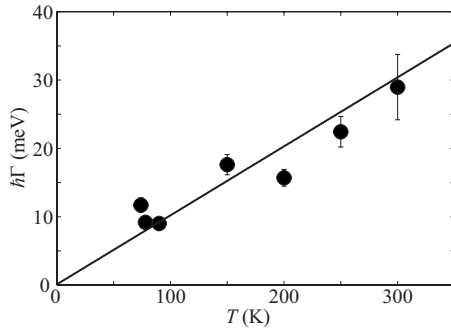
FIG. 3. T dependence of the spin relaxation rate derived from the global fitting analysis described in the text. The solid line shows the best straight line fit, $\hbar\Gamma = \mathcal{C}k_B T$ with $\mathcal{C}=1.17(9)$.

pinch points,[25] which again may not be detectable in powder data. While the theory is not relevant for the ordered state, the close correspondence with the measurements here indicate similarities in local dynamic correlations across the phase transition.

Although the Q dependence of the data does not change appreciably below room temperatures Fig. 2 shows substantial changes in the fluctuation spectrum. Above T_N the spectra are well described [solid line in Figs. 2(a) and 2(b)] by the response function $\chi''(\omega)=\chi_0\omega\Gamma/(\Gamma^2+\omega^2)$, which is related to the neutron scattering spectrum through the fluctuation dissipation theorem.[28] Factorization of the Q and ω dependence of the cross section was assumed so Γ characterizes the local response. The T dependence of the relaxation rate (Fig. 3) is described by $\hbar\Gamma = \mathcal{C}k_B T$ where $\mathcal{C}=1.17(9)$, allowing for a constant-Γ_0 term gives $\Gamma_0=3(1)$ meV and $\mathcal{C}=0.8(1)$. Linear-in-T dependence of Γ was previously found in simulation of classical Heisenberg spins with AFM interactions on a pyrochlore lattice.[3] A spin fluctuation rate close to $k_B T$ was also observed in the frustrated spinel systems $ZnCr_2O_4$ and LiV_2O_4.[10,26]

For $T < T_N$ a gap appears in the excitation spectra as spectral weight moves to higher energy [Figs. 2(c) and 2(d)]. At $T=15$ K the neutron data indicate an energy gap $\Delta=11(1)$ meV. This is significantly less than the 23 meV gap inferred from specific heat data, which may be dominated by activation of the modes associated with the 19.7 meV peak.[17] A gapped spectrum was confirmed by the normalized higher-resolution DCS data which, integrated over energies from 2 to 8 meV, show no evidence of spin waves emanating from the AFM Bragg peaks [solid squares in Fig. 2(h)] as in $ZnCr_2O_4$.[10] When a phase transition breaks a continuous symmetry, Goldstone's theorem assures gapless excitations. The observation of a spin gap in $Y_2Ru_2O_7$ is, however, consistent with both easy-plane and easy-axis anisotropy. This is because easy planes in the pyrochlore structure by symmetry are not parallel. Hence no global rotation can maintain spins in easy planes.[27]

Having examined both the high-T critical state and the low-T ordered state, we focus on the transition between these phases. Figure 4 compares the T dependence of the inelastic peak position to the integrated intensity of the (111) Bragg reflection. Apart from probing the staggered magnetization squared, the (111) reflection has a small nuclear component
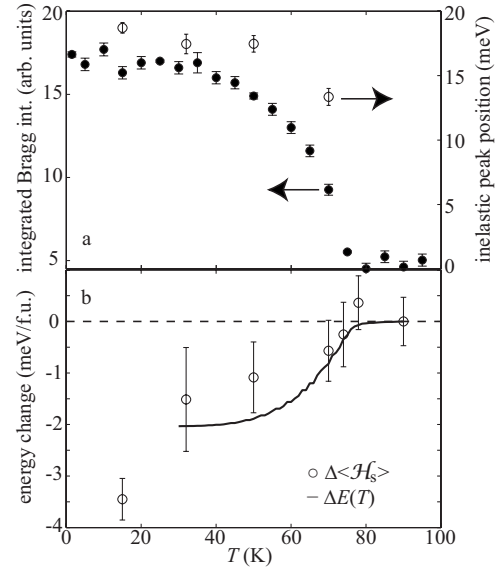

FIG. 4. (a) T dependence of the integrated intensity of the (111) Bragg peak (●) which has nuclear and magnetic contributions. (○) Indicates the position of the inelastic peak in the spectrum, derived by fits described in the text. (b) Results of the first moment analysis described in the text. (○) indicates the change in spin exchange energy, while the solid line denotes the overall change in energy obtained by integrating specific heat data (Ref. 17).

and therefore does not vanish for $T > T_N$.[18] The inelastic peak position was obtained by fitting a damped harmonic oscillator response[28] to the $0.8 \leq Q \leq 1.4$ Å^{-1} integrated part of the excitation spectra. While the inelastic peak moves to lower energies upon heating (see Fig. 4) it is important to note that a finite-energy peak persists for $T=T_N$. This indicates that short-range dynamic correlations at T_N are sufficient to maintain a distinct spectral maximum in the excitation spectrum.

The shift of spectral weight from a relaxation response towards higher energies implies that the energy of the spin system, $\langle\mathcal{H}_s\rangle$, is reduced through the phase transition. This can be quantified using normalized inelastic magnetic neutron scattering data and the first moment sum rule[10,29]

$$\Delta\langle\mathcal{H}_s\rangle = -\frac{3}{2}\frac{\hbar^2\int_0^\infty \omega(1-e^{-\beta\hbar\omega})\Delta S(Q,\hbar\omega)d\omega}{1-\sin Qd/Qd}. \quad (1)$$

Here we consider only the isotropic nearest-neighbor interaction between spins separated by a distance d. A more complete expression that includes anisotropy terms can readily be derived[28] but the quality of the present data do not warrant the added complexity. Limiting the integral to 5 to 30 meV and averaging data for $0.8 < Q < 1.4$ Å^{-1}, the temperature variation of the spin energy $\Delta\langle\mathcal{H}_s\rangle$ relative to the value at $T=90$ K is shown as open circles in Fig. 4(b). The data can be compared to the overall change in energy obtained from the magnetic specific heat,[17] $\Delta E(T) = \int_0^T C_m(T')dT' - \int_0^{T_{max}} C_m(T')dT'$, shown as a solid line in Fig. 4(b). While most of the variation in the thermal energy is accounted for by $\Delta\langle\mathcal{H}_s\rangle$ and no structural changes have

been observed at the transition, the relatively large error bars leave room for an increase in the lattice energy below T_N by up to 1.5(5) meV/f.u. Note also that spin-phonon coupling was detected through an anomaly in the temperature dependence of a Raman-active mode frequency at T_N.[30]

While all known pyrochlore antiferromagnets show some form of (intrinsic or extrinsic) static correlations for sufficiently low T, only $Y_2Ru_2O_7$ and its derivatives feature second-order phase transitions to long-range Néel order. The apparent lack of involvement of lattice degrees of freedom indicates that this is a true magnetic instability the understanding of which may require a different frame work than for $ZnCr_2O_4$. The apparent gap in the excitation spectrum indicates that spin space anisotropy may be significant. While we detect the magnitude of the gap there is no direct information about the magnitude or nature of any spin space anisotropic terms in the Hamiltonian. The fact that the gap mode is relatively sharp in energy for a powder sample indi-

cates that the corresponding excitations are weakly dispersive and this points to local soft modes pushed to a finite energy on account of quantum fluctuations. Indeed the first moment analysis of $\widetilde{S}(Q, \omega)$ shows that the energy gain associated with ordering is intimately related to the development of the 19.7 meV peak. The principal challenge posed by our experiment is thus to understand the interplay between quantum fluctuations and anisotropy terms in establishing the Néel state spin gap and spin resonance in the frustrated pyrochlore AFM.

---

[1] J. E. Greedan, J. Mater. Chem. **11**, 37 (2001).

[2] P. W. Anderson, Phys. Rev. **102**, 1008 (1956).

[3] R. Moessner and J. T. Chalker, Phys. Rev. Lett. **80**, 2929 (1998).

[4] C. L. Henley, Phys. Rev. B **71**, 014424 (2005).

[5] S. V. Isakov, K. Gregor, R. Moessner, and S. L. Sondhi, Phys. Rev. Lett. **93**, 167204 (2004)

[6] O. Tchernyshyov, R. Moessner, and S. L. Sondhi, Europhys. Lett. **73**, 278 (2006).

[7] J. S. Gardner, B. D. Gaulin, S.-H. Lee, C. Broholm, N. P. Raju, and J. E. Greedan, Phys. Rev. Lett. **83**, 211 (1999).

[8] J. S. Gardner, A. Keren, G. Ehlers, C. Stock, E. Segal, J. M. Roper, B. Fåk, M. B. Stone, P. R. Hammar, D. H. Reich, and B. D. Gaulin, Phys. Rev. B **68**, 180401(R) (2003).

[9] Y. Machida, S. Nakatsuji, Y. Maeno, T. Tayama, T. Sakakibara, and S. Onoda, Phys. Rev. Lett. **98**, 057203 (2007).

[10] S.-H. Lee, C. Broholm, T. H. Kim, W. Ratcliff, II, and S.-W. Cheong, Phys. Rev. Lett. **84**, 3718 (2000).

[11] O. Tchernyshyov, R. Moessner, and S. L. Sondhi, Phys. Rev. B **66**, 064403 (2002).

[12] R. Kanno, Y. Takeda, T. Yamamoto, Y. Kawamoto, and O. Yamamoto, J. Solid State Chem. **102**, 106 (1993).

[13] S. Yoshii and M. Sato, J. Phys. Soc. Jpn. **68**, 3034 (1999).

[14] J. Park, K. H. Kim, H.-J. Noh, S.-J. Oh, J.-H. Park, H.-J. Lin, and C.-T. Chen, Phys. Rev. B **69**, 165120 (2004).

[15] H. Sakai, H. Kato, S. Kambe, R. E. Walstedt, H. Ohno, M. Kato, K. Yoshimura, and H. Matsuhata, Phys. Rev. B **66**, 100509(R) (2002).

[16] N. Tiara, M. Wakeshima, and Y. Hinatsu, J. Solid State Chem. **152**, 441 (2000).

[17] M. Tachibana, H. Kawaji, and T. Atake, Phys. Rev. B **71**, 060402(R) (2005).

[18] M. Ito, Y. Yasui, M. Kanada, H. Harashina, S. Yoshii, K. Murata, M. Sato, H. Okumura, and K. Kakurai, J. Phys. Soc. Jpn. **69**, 888 (2000); M. Ito, Y. Yasui, M. Kanadaa, H. Harashinaa, S. Yoshii, K. Murata, M. Sato, H. Okumura, and K. Kakurai, J. Phys. Chem. Solids **62**, 337 (2001).

[19] M. W. Johnson, Harwell Report No. AERE-R7682, 1974 (unpublished).

[20] P. J. Brown, in *International Tables for Crystallography*, edited by A. J. C. Wilson (Kluwer, London, 1995), Vol. C.

[21] S. W. Lovesey, *Theory of Neutron Scattering from Condensed Matter* (Clarendon Press, Oxford, 1984).

[22] S.-H. Lee, C. Broholm, W. Ratcliff, G. Gasparovic, Q. Huang, T. H. Kim, and S.-W. Cheong, Nature (London) **418**, 856 (2002).

[23] O. Tchernyshyov, R. Moessner, and S. L. Sondhi, Phys. Rev. Lett. **88**, 067203 (2002).

[24] U. Hizi and C. L. Henley, J. Phys.: Condens. Matter **19**, 145268 (2007).

[25] S. Yoshida, K. Nemoto, and K. Wada, J. Phys. Soc. Jpn. **71**, 948 (2002).

[26] S.-H. Lee, Y. Qiu, C. Broholm, Y. Ueda, and J. J. Rush, Phys. Rev. Lett. **86**, 5554 (2001).

[27] L. Balents (private communication).

[28] I. Zaliznyak and S.-H. Lee, in *Modern Techniques for Characterizing Magnetic Materials*, edited by Y. Zhu (Springer, Heidelberg, 2005).

[29] P. C. Hohenberg and W. F. Brinkman, Phys. Rev. B **10**, 128 (1974).

[30] J. S. Bae, I.-S. Yang, J. S. Lee, T. W. Noh, T. Takeda, and R. Kanno, Phys. Rev. B **73**, 052301 (2006).